Synthesis and characterization of nanostructured ternary composites of graphene oxide/Fe₃O₄/NiO for waste water treatment

T. Saleem[a], R. A. Sarfaraz[a], I. Ahmed[b], H. Zulfiqar[b], Y. Iqbal[b,c], I. Saeed[a], M. Ashraf[a], U. Anwar[d,*]
[a]Department of Chemistry, University of Agriculture Faisalabad-38030, Pakistan
[b]Department of Chemistry, Government College University Faisalabad-38000, Pakistan
[c]Department of Chemistry, University of Sialkot-51040, Pakistan
[d]Soochow Institute for Energy and Materials Innovations, College of Energy, Soochow University, Suzhou 215006, China

Photocatalysis using solar energy and semiconductors is widely used in the purification of air and the processing of wastewater. Present study deal with cost-effective GO synthesis, supporting NiO/Fe₃O₄ ternary nanocomposites; for the rapid photocatalytic degradation of the Rhodamine B Dye. For this purpose, nickel oxide nanoparticles and iron oxide nanoparticles were synthesized by hydrothermal method. Synthesis of graphene oxide was done by using modified hummers method. These trimetallic nanoparticles were characterized by FTIR (Fourier Transform Infrared Spectroscopy), Scanning Electron Microscopy (SEM) and X-ray Diffraction Crystallography (XRD) for structure, shape and composition determination. The photocatalytic degradation of Rhodamine B dye was conducted and various parameters like catalyst amount, dye concentration, pH and contact time optimization were performed to evaluate dye degradation efficiency of Fe₃O₄/NiO/Graphene trimetallic nanoparticles. Kinetic models were studied to check degradation rate and Pseudo 1st order kinetic model was most suitable to the experimental data of dye degradation.

1. Introduction

Solar-driven catalytic reaction is seen as a promising way to address current ecological and fuel challenges. [1, 2].Photocatalytic deterioration of organic contaminants is among the simple, cheap, clean, and ecofriendly methods being deployed [3, 4]. Better separation of electron and hole has been shown to have a key role in enhancing photocatalytic performance.[5, 6]. Semiconductor materials, for example iron oxide and nickel oxide, considered effective photocatalysts for ecological cleanup when exposed to sunshine. [7, 8]. Iron oxide nanoparticle consist of maghemite (Fe₂O₃) or magnetite (Fe₃O₄) particle and has potential applications in electromagnetic data collection, bioimaging, drug-delivery etc.[9]**.**

Iron oxide nanoparticles have drawn significant attention mainly due to presence of superparamagnetic characteristics and their possible biotechnological applications resulting from its corrosion resistance and non-toxicity [10]. Magnetite (Fe₃O₄) has received significant interest among numerous magnet nanomaterials, given its huge potential in terms of cost efficiency, environmentally friendly design, super paramagnetism, non - toxicity, good absorption properties and special optochemical characteristics. Iron oxide nanoparticles do however have a very narrow band gap (0.1 eV) and are easy to excite them in the sun [11]. Nickel oxide is an intermediate in manufacture of alloy-nickel with the NiO formula known as a simple metal oxide. Nickle oxide has various specialized applications, including lithium-ion anode, alkaline battery cathode

---

products, solar cell sensing, active gas layer sensor, electrochromatic coating, electrical and chemical supercapacitors. Many efficacious techniques, primarily sol-gel, co-precipitation, thermal sonochemical decomposition were designed for the preparation of NiO nanostructures [12].

Graphene is considered to be the most strong and smallest compound ever known and its structural features like the crosslinks between layers or the Van-Der Waals influences contribute to these features. Graphene-based nanocomposites are also excellent materials for the catalyst support when catalytic activities are carried out because they increase the durability and surface area of enzyme. Graphene compositions with several other nanomaterials use its superior properties to boost catalytic activity [13]. The nanostructural morphology and photochemical properties of graphene oxide–metal oxide compared to graphene oxide indicate strong candidates for treatment projects [14]. Due to its unique properties, graphene has emerged as a potential candidate for its use in composite materials. Researchers are involved in studying nanocomposites based on graphene and, in particular, graphene based metal oxides, leads to distinct applications [12].

In this study Fe3O4/NiO/GO nanocomposite were newly constructed and used as a photocatalyst. The prepared photocatalyst is used for effective degradation of rhodamine B dye. The degradation was gone to 97% after 100 min.

2. Experimental section

2.1. Materials
All chemicals and organic solvents etc. are of high impurity, and no further purification is needed.

2.2. Synthesis of Iron Oxide nanoparticles
Iron oxide (Fe_3O_4) nanoparticles were synthesized by hydrothermal method. For fabrication of nanoparticles 1 g of ferrous chloride hydrated ($FeCl_2.4H_2O$) were added into the beaker containing 50mL distilled water while continuously stirring at moderate speed. Then 32% of liquid ammonium hydroxide (NH_3OH) was added to the reaction mixture dropwise till it reached at 11 pH. At this stage solution has black color. After this 20% hydrazine solution was added into the solution. Further on addition of 4 to 5 drops of 3% solution of polyvinyl alcohol (PVA) as stabilizing agent to the reaction mixture. Then the solution was transfer from beaker to the autoclave and sealed it. It was heated at 180°C for 8 hours. After cooling of the autoclave obtained precipitate was centrifuged at 3000 rpm and washed four times with water and once with ethanol to maintain neutral pH and removal of unreacted salts. Then precipitates were shifted into petri dish and dried in oven at 50°C. Then precipitates were kept in crucible and calcined at 500°C for 3 hours [15].

2.3. Synthesis of nickel oxide nanoparticles
Nickel oxide nanoparticles were synthesized by hydrothermal method. For fabrication of nanoparticles 1 g of nickel chloride hydrated ($NiCl_2.6H_2O$) were added into the beaker containing 50mL distilled water while continuously stirring at moderate speed. Then 1M solution of liquid sodium hydroxide (NaOH) was added to the reaction mixture dropwise till it reached at 11 pH. At this stage solution color has changed from green to purple. After this 20% hydrazine solution was added into the solution. Further on addition of 4 to 5 drops of 3% solution of polyvinyl alcohol (PVA) as stabilizing agent to the reaction mixture. Then the solution was transfer from beaker to the autoclave and sealed it. It was heated at 180°C for 8 hours. After cooling of the autoclave obtained precipitate was centrifuged at 3000 rpm and washed four times with water and once with ethanol to maintain neutral pH and removal of unreacted salts. Then precipitates were shifted into petri dish and dried in oven at 50°C. Then precipitates were kept in crucible and calcined at 500°C for 3 hours [16].

2.4. Synthesis of graphene oxide (GO)

For the preparation of graphene oxide, mixing of 1.5g of graphite powder and 0.75g of sodium nitrate (NaNO$_3$) was done in 60ml of concentrated sulphuric acid by constant stirring on hotplate. Then 60ml of concentrated sulphuric acid was added dropwise in beaker and vigorous stirring was done for 30 minutes. This made the solution color black. Then made an ice bath and 7g of KMnO$_4$ was added in beaker pinch by pinch by constant stirring for 1 hour until green color was appeared. After this sample beaker was kept in water bath and temperature of water bath was maintained upto 37°C. Stirring had done continuously until brown color appeared in hot plate. After this made an oil bath and temperature of oil bath was kept up to 96-98°C. 63ml of distilled water was added dropwise by continuous stirring. Then 10ml of H$_2$O$_2$ will be added until yellowish brown color appeared. This yellowish brown material was dried in oven at 70°C temperature to obtain graphene sheet [17].

Graphene was reported as an excellent reinforcement material that stabilizes various nanostructures [18]. Survey study exposed that in order to acquire unique characteristics in synthesizing material; graphene was synthesized using Hummer's method [19].

2.5. Synthesis of Fe$_3$O$_4$/NiO/GO nanocomposite

The facile and green hydrothermal method was carried out for the fabrication of Fe$_3$O$_4$/NiO/GO nanocomposite. In this experiment, 2 g of graphene oxide (GO) was dispersed in 50 ml of distilled water through sonication for 1 hour. 1 g of synthesized iron oxide nanoparticles as well as nickel oxide nanoparticles were added into the graphene solution under constant stirring for another I hour. Then neutralize the pH of mixture/solution of Fe$_3$O$_4$/NiO/GO nanocomposite. The resulting solution was transferred into 100 ml Teflon-lined stainless-steel autoclave and kept in oven at 160 °C for 6 hours. Eventually, obtained black precipitates were washed through centrifugation using water and methanol. Final product was obtained by drying the sample in an oven at 60°C temperature for 24 hours(Fig.1). It was reported that graphene reinforced iron and nickel oxide nanocomposites were synthesized via chemical method [20].
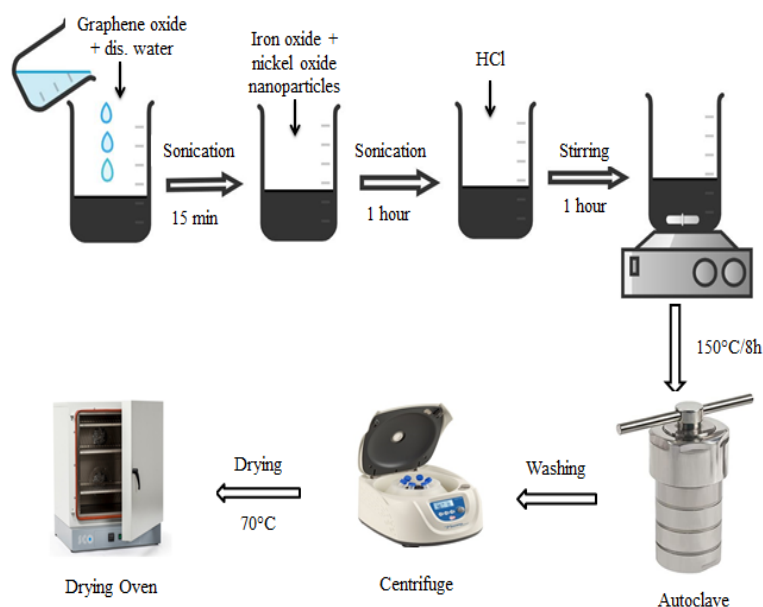

Fig.1. Synthesis of Nanocomposite.

2.6. Photocatalytic Activity

The photocatalytic performance as synthesized Fe$_3$O$_4$/NiO/GO nanocomposite was checked against rhodamine B dye. To study dye removal without control experiments (dye solution/sunlight and photocatalyst addition, solution/H$_2$O$_2$/sunlight) were also performed to get better degradation outcomes. In dye degradation experiment 20 mg of Fe$_3$O$_4$/NiO/GO

nanocomposite was added in 20 mL of Rhodamine B dye solution where graphene modified the surface of iron and nickel nanoparticles and improves its reduction efficiency. The optimum Ph for this reaction was 3 and time was 100 minto get 97% degradation efficiency The percentage degradation was estimated according to the following equation;

$$Percentage\ degradation = (Co\text{-}Ct/\ Co)\ 100$$

where Co is the initial absorbance of the dye before mixing with the catalyst and reaction time (t-0), whereas Ct is the absorbance of the dye after addition of catalyst and after given reaction time (t=t).

3. Results and Discussion

3.1. Morphology

The particle size and surface morphology of the Fe_3O_4/NiO/GO hybrid nanocomposite were examined by Field Emission Scanning Electron Microscope by Department of Chemistry, Government College University, Faisalabad. Figure 2 shows the analysis of Fe_3O_4/NiO/GO hybrid nanocomposite at three different magnifications range. Small nanosized cubic iron oxide and nickel oxide nanoparticles have covered the graphene surface densely, showing their dispersion into graphene sheets. There was also a high tendency of agglomerations. The particle agglomeration reduces the interfacial surface and surface area which causes the particle adhesion with each other because of the wander wall forces. The hybrid nanocomposite comprising cubic iron oxide (Fe_3O_4) and nickel oxide (NiO) nanoparticles and graphene sheets (GO) is confirmed by SEM examination.
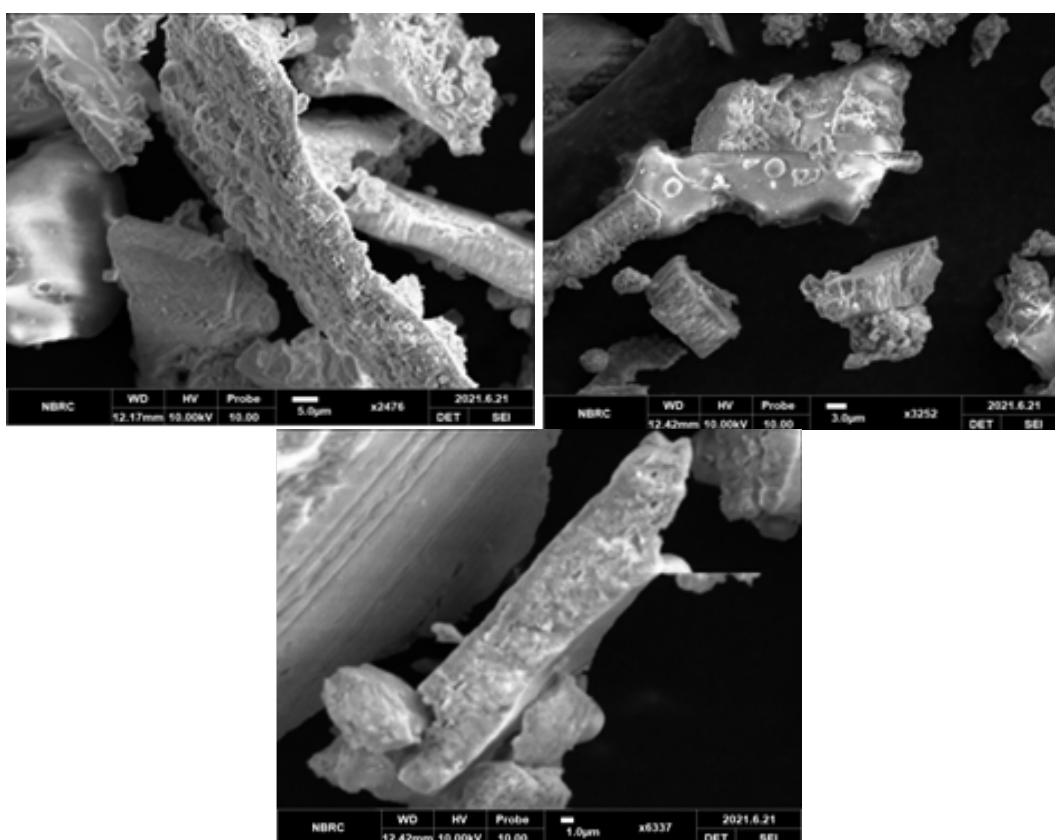

Fig. 2. SEM image of Fe_3O_4/NiO/GO hybrid nanocomposite.

3.2. Composition and structural information

XRD was used to determine the crystallinity and purity of the hybrid nanocomposite as it was produced. (Fig.3a)These six peaks correspond to crystal planes (220), (400), (311), (422), (440) and (511) of Fe_3O_4 with a cubic spinal structure. No additional impurities were detected in these peaks, which verified the existence of Fe_3O_4 with a cubic spinal structure. Due to the tiny size of the NiO nanoparticles, the XRD peaks were intense and wide. In the hybrid nanocomposites, the peak locations were given to the (111), (220), (200), (222) and (311). In accordance with the standard JCPDF No. 04-0835, all the peaks were assigned to the face centered cubic (FCC) crystalline structure of NiO. Fe_3O_4 and NiO incorporation in graphene sheets were verified by XRD. There were no additional impurities found in the XRD pattern, with the exception of the typical peaks of the FCC phase NiO and Fe_3O_4 spinal structure.

The FTIR (Fourier Transform Infrared Spectroscopy) as shown in (Fig.3b) spectrum of Fe_3O_4/NiO/GO nanocomposite represents the three absorption bands at $1045cm^{-1}$, 1730 cm^{-1}, and $1624cm^{-1}$ attributed to C-O (alkoxy), C=O (carbonyl) and C=C stretching vibrations of graphene oxide, respectively. A broad peak at $3494cm^{-1}$ is distinct peak of H-O-H stretching vibration, which is due to the absorbed water. Fe-O stretching peak is observed at $594cm^{-1}$ indicating the successful deposition of iron oxide on graphene sheet. Stretching frequency peak of C-H band is observed at $3290cm^{-1}$. In the process of reduction by hydrazine, it has been revealed that most of the functional groups carrying oxygen has now been eliminated from GO and therefore essentially turned into graphene.
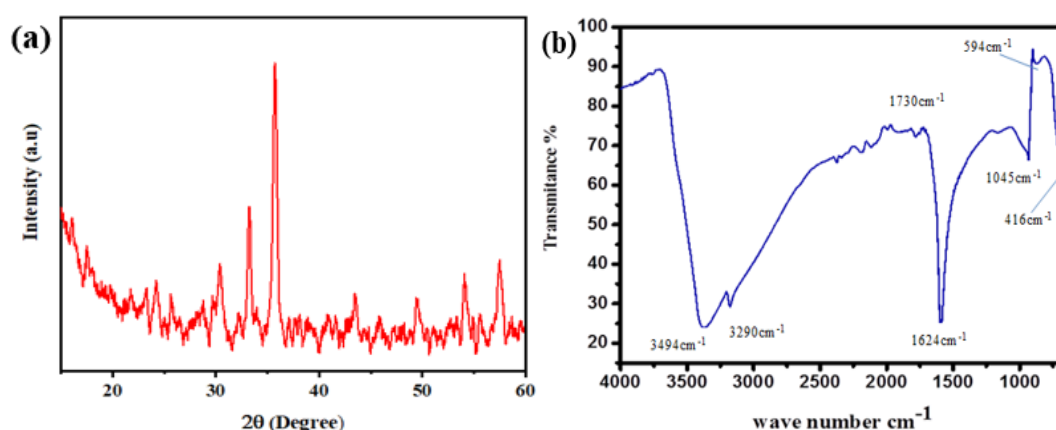

Fig. 3. (a) XRD patterns (b) FT-IR patterns of (Fe_3O_4/NiO/GO) ternary composite.

3.3. Photocatalytic degradation of rhodamine B

The photocatalytic degradation of rhodamine b dye was carried out in sunlight and no reaction in absence of catalyst or sunlight. When rhodamine B dye is exposed to sunlight the degradation is started. The rate of degradation is fast at the start of reaction and it decays as time passes.Fig.4a indicating the degradation of rhodamine b dye over (Fe_3O_4/NiO/GO) ternary composite followed the pseudo first kinetics, $\ln (C^0/C) = kt$, where C0 and C are the initial and time t of the rhodamine b solution respectively, and k is rate constant. The results revealed that after 100 min the degradation efficiency goes up to 97%. The excellent photocatalytic activity may be due to two reasons: (i) good absorption of visible light (ii) decrease band gap energy that can enhance the transfer of photo-induce electron and decrease the electron hole recombination.
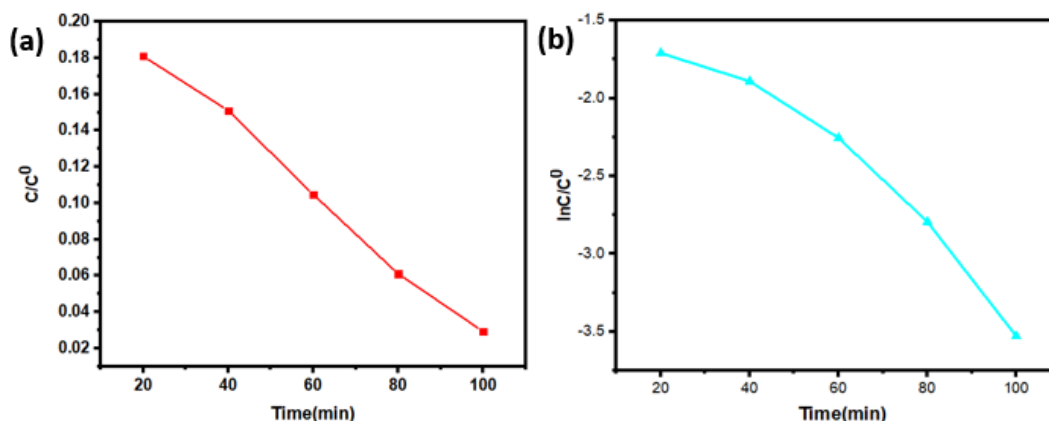
Fig.4. (a)Photocatalytic degradation of rhodamine b with (Fe₃O₄/NiO/GO) ternary composite;
(b) First order Kinetics

The optimization of reaction parameters was also done by different experiments. Fig. 5a showed the Degree of dye photodegradation got intensified by increasing the amount of Fe_3O_4/NiO/GO nano catalyst, which raised up to 35 mg of dose amount and beyond this, dye photodegradation did not raised significantly. This is because at higher catalyst amount, then increasing the number of active sites on the surface of the catalyst. So, in this way the number of radicals also increased. At the optimum dose of catalyst enhances the reaction sites and also increased the radical's synthesis ($OH^·$). The insignificant photocatalytic activity (PCA) at higher catalyst dose can be compared with aggregation of Fe_3O_4/NiO/GO nanocomposite because at increased amounts of catalyst dose, surface area was also minimized. As a result, photocatalytic activity was reduced. As shown in below Fig 5b the influence of pH on photocatalytic activity for dye degradation was optimistic and indicated highest degradation at pH 3. The percentage (%) degradation was significantly decreased as pH moved from acidic to basic and after that, reduction at basic pH range was observed. Consequently, pH 3 was found as optimized pH for Rhodamine B dye degradation because the production of OH radicals become higher at pH 3 while lower at above pH value. The Rhodamine B dye photodegradation increased linearly with respect to time as shown in Fig.5c and then reached at maximum after 100 min of irradiation time. This increased rate of dye removal was due to higher availability of active sites on nanocomposite's surface and beyond this; the reduction in Rhodamine B dye photodegradation might be because of the coverage of most active sites of nanocomposite catalyst with dye molecules which leads to prevent the catalyst from undegraded dye molecules.Fig. 5d indicate that in the presence of oxidant(H_2O_2), using Fe_3O_4/NiO/GO nanocomposite (catalyst) showed highest degradation of Rhodamine B dye (91 %) in 45 min while in the absence of H_2O_2, catalyst displayed maximum degradation of Rhodamine B dye at 86 % in 60 min. The H_2O_2 concentration was varied as 3, 5, 7, 9, and 11 mM. The maximum deterioration of Rhodamine B dye was observed at 7 mM concentration. As a result, it was concluded that oxidant fastens the degradation process of dye. It affects the reaction rate of photocatalytic degradation.
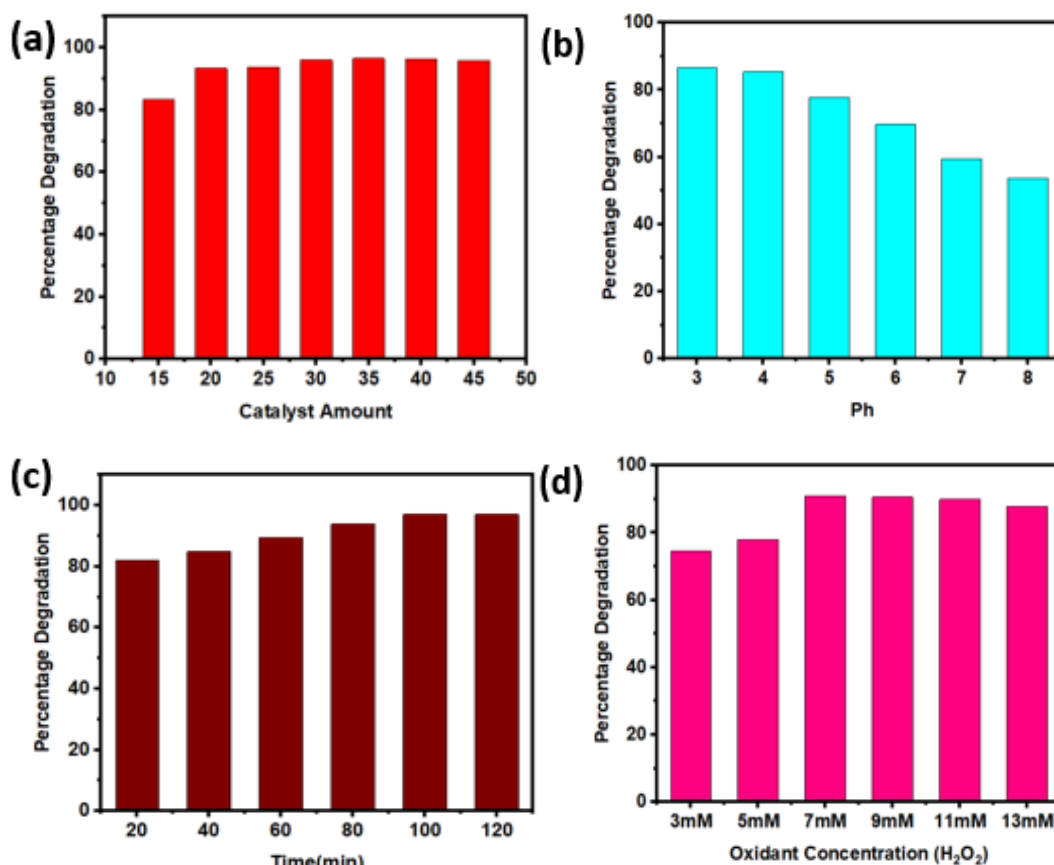
Fig.5. Optimization of (a)time, (b) Ph, (c) time using (Fe₃O₄/NiO/GO) ternary composite (d) Degradation efficiency using Oxidant (H₂O₂).

4. Conclusion

In current work study, modified Hummer's method was applied to fabricate graphene oxide, iron oxide NPs and nickel oxide NPs were synthesized by hydrothermal process. The degradation efficiency of Fe_3O_4/NiO/GO nanocomposite was evaluated. The structural profiles as well as size of synthesized Nano catalyst were investigated using different characterization techniques like SEM, FT-IR, Ultraviolet-Visible spectrophotometer and XRD. X-Ray Diffraction assists for seeing crystalline morphology, degree of crystallinity, crystal lattice structure and atomic spacing within the crystal. The SEM analysis helps to determine the surface morphology of NPs. Various functional groups (FG) were confirmed via FTIR analysis while maximum absorbance wavelength was checked via UV-Visible spectra.

The photocatalytic degradation performance of iron oxide/nickel oxide/graphene nanocomposite was observed by photodegradation of Rhodamine B dye under solar irradiation and various degradation parameters such as catalyst dose, dye concentration, time and pH were also optimized. In the degradation process using iron oxide/nickel oxide/graphene nanocomposite, the pH 3, catalyst dose 35mg and time duration 100 min were optimized for highest percentage degradation. Kinetically, the photocatalytic degradation followed the Pseudo-first-order kinetic model. All the obtained results exposed that iron oxide/nickel oxide/graphene nanocomposite could be easily applied for the complete photocatalytic deterioration of Rhodamine B dye at industrial level.

References

[1] Bhatkhande. S, Pangarkar, Beenackers.A, Journal of Chemical Technology & Biotechnology 77(1) 102 (2002); https://doi.org/10.1002/jctb.532

[2] Sanakousar, F., et al., Materials Science in Semiconductor Processing 140 106390 (2022); https://doi.org/10.1016/j.mssp.2021.106390

[3] Karthik, K., et al., Chemosphere 287 132081 (2022); https://doi.org/10.1016/j.chemosphere.2021.132081

[4] Dai, Z., et al., Digest Journal of Nanomaterials & Biostructures (DJNB) 17(1) (2022)

[5] Al-Hamoud, K., et al., ACS omega 7(6) 4812 (2022); https://doi.org/10.1021/acsomega.1c05090

[6] Liu, M., et al., Journal of Alloys and Compounds 905 16402 (2022); https://doi.org/10.1016/j.jallcom.2022.164246

[7] Ali, T., et al., Ceramics International 48(6) 8331 (2022); https://doi.org/10.1016/j.ceramint.2021.12.039

[8] Roostaee, M. and I. Sheikhshoaie., Environmental Research 205 112510 (2022); https://doi.org/10.1016/j.envres.2021.112510

[9] Bagheri, S. and N.M. Julkapli., Reviews in Inorganic Chemistry 36(3) 135 (2016); https://doi.org/10.1515/revic-2015-0014

[10] Abdullah, N.H., et al., Composites Part B: Engineering 162 538 (2019); https://doi.org/10.1016/j.compositesb.2018.12.075

[11] Vinodhkumar, G., et al., Physica B: Condensed Matter 580 411752 (2020); https://doi.org/10.1016/j.physb.2019.411752

[12] Soofivand, F. and M. Salavati-Niasari., Journal of Photochemistry and Photobiology 337 44 (2017); https://doi.org/10.1016/j.jphotochem.2017.01.003

[13] Olatunde.O and Onwudiwe., International journal of environmental research and public health 18(4) 1529 (2021); https://doi.org/10.3390/ijerph18041529

[14] El-Shafai, N., et al., RSC Advances 8 (2018); https://doi.org/10.1039/C8RA00977E

[15] Sirajudheen, P., et al., Surfaces and Interfaces 21 100640 (2020); https://doi.org/10.1016/j.surfin.2020.100648

[16] Vengatachalam, M., et al., Asian Journal of Chemistry 33 411 (2021)

[17] Loryuenyong, V., et al., Advances in Materials Science and Engineering 1 (2013); https://doi.org/10.1155/2013/923403

[18] Hu, Z., et al., Materials Science and Technology 32 930 (2016); https://doi.org/10.1080/02670836.2015.1104018

[19] Zaaba, N.I., et al., Procedia Engineering 184 469 (2017); https://doi.org/10.1016/j.proeng.2017.04.118

[20] Shanmugam, M. and Y. Ahn., New Journal of Chemistry 42 (2018)